Journal of Bioscience and Bioengineering
VOL. xx No. xx, 1–5, 2014

www.elsevier.com/locate/jbiosc

# $^{13}$C-based metabolic flux analysis of *Saccharomyces cerevisiae* with a reduced Crabtree effect

Shuichi Kajihata,[1] Fumio Matsuda,[1] Mika Yoshimi,[1] Kenshi Hayakawa,[2] Chikara Furusawa,[1,3] Akihisa Kanda,[4] and Hiroshi Shimizu[1,*]

*Department of Bioinformatic Engineering, Graduate School of Information Science and Technology, Osaka University, 1-5 Yamadaoka, Suita, Osaka 565-0871, Japan,[1] KANEKA Fundamental Technology Research Alliance Laboratories, Graduate School of Engineering, Osaka University, 2-8 Yamadaoka, Suita, Osaka 565-0871, Japan,[2] Quantitative Biology Center, RIKEN, 6-2-3 Furuedai, Suita, Osaka 565-0874, Japan,[3] and New & Fundamental Technology Group Process Technology Laboratories, KANEKA Corporation, 1-8 Miyamae-cho, Takasago-cho, Takasago, Hyogo 676-8688, Japan[4]*

Received 27 August 2014; accepted 15 December 2014
Available online xxx

***Saccharomyces cerevisiae* shows a Crabtree effect that produces ethanol in a high glucose concentration even under fully aerobic condition. For efficient production of cake yeast or compressed yeast for baking, ethanol by-production is not desired since glucose limited chemostat or fed-batch cultivations are performed to suppress the Crabtree effect. In this study, the $^{13}$C-based metabolic flux analysis ($^{13}$C-MFA) was performed for the S288C derived *S. cerevisiae* strain to characterize a metabolic state under the reduced Crabtree effect. *S. cerevisiae* cells were cultured at a low dilution rate (0.1 $h^{-1}$) under the glucose-limited chemostat condition. The estimated metabolic flux distribution showed that the acetyl-CoA in mitochondria was mainly produced from pyruvate by pyruvate dehydrogenase (PDH) reaction and that the level of the metabolic flux through the pentose phosphate pathway was much higher than that of the Embden–Meyerhof–Parnas pathway, which contributes to high biomass yield at low dilution rate by supplying NADPH required for cell growth.**



[**Key words:** $^{13}$C-based metabolic flux analysis; Crabtree effect; Central carbon metabolism; *Saccharomyces cerevisiae*; Redox balance]

*Saccharomyces cerevisiae* is an industrial microorganism with stable ethanol fermentation performance even under aerobic and high glucose concentration conditions (1). The Crabtree effect is, however, not preferable to efficiently produce cake yeast or compressed yeast for baking because glucose-limited chemostat or fed-batch cultivation is required to suppress ethanol by-production. While baker's yeasts are industrially produced at a specific growth rate of 0.25 $h^{-1}$ for faster cell growth, it has been reported that no ethanol production by the Crabtree effect occurs in a glucose-limited culture with dilution rates of approximately 0.1–0.15 $h^{-1}$ (2). Previous studies suggested that the limited respiratory capacity of *S. cerevisiae* mitochondria is countered by the Crabtree effect to maintain the redox balance in the cytosol (3,4).

To further characterize the metabolic state related to the Crabtree effect, $^{13}$C-based metabolic flux analysis ($^{13}$C-MFA) was conducted using *S. cerevisiae* ATCC 32167 strain (2). The glucose limited chemostat cultivations showed that a Crabtree effect was observed at dilution rates of 0.30 $h^{-1}$ and 0.40 $h^{-1}$ that had ethanol yields of 0.16 and 0.36 C-mol C-mol-glucose$^{-1}$, respectively. The metabolic flux analysis at a dilution rate of 0.40 $h^{-1}$ revealed that the flux level of the Embden–Meyerhof–Parnas (EMP) pathway (77.9 when the glucose uptake rate was set to 100) was larger than that of the pentose phosphate (PP) pathway (15.1 relative to the glucose uptake rate). In the case of a dilution rate of 0.15 $h^{-1}$, no ethanol production by the Crabtree effect was observed, and the biomass yield from the glucose was increased to 0.57 C-mol C-mol-glucose$^{-1}$, which is twice as high as the yield with a dilution rate of 0.40 $h^{-1}$ (0.29 C-mol C-mol-glucose$^{-1}$) (2). The metabolic flux level of the EMP pathway was reduced to 25.2 and that of PP pathway was increased to 54.7. This result suggests that the activation of the PP pathway should relate to the reduced Crabtree effect in the ATCC 32167 strain.

The $^{13}$C-MFA study also suggested a metabolic route for mitochondrial acetyl-CoA supply in the presence of a reduced Crabtree effect. The metabolic flux analysis revealed that mitochondrial acetyl-CoA was dominantly supplied from mitochondrial pyruvate by pyruvate dehydrogenase (PDH) in the fermentative growth condition ($\mu$ = 0.40 $h^{-1}$). The metabolic flux of the PDH reaction was determined to be 23.7 relative to the glucose uptake rate when the glucose uptake rate was set to 100. In the oxidative condition ($\mu$ = 0.15 $h^{-1}$), intercompartmental acetyl-CoA transport was the major route for mitochondrial acetyl-CoA supply (53.4). In this pathway, pyruvate was first decarboxylated to acetaldehyde by pyruvate decarboxylase (PDC), which was converted to acetate and acetyl-CoA in the cytosol, and then transported into the

* Corresponding author. Tel./fax: +81 6 6879 7446.
*E-mail addresses:* s-kajihata@ist.osaka-u.ac.jp (S. Kajihata), fmatsuda@ist.osaka-u.ac.jp (F. Matsuda), mika_yoshimi@bio.eng.osaka-u.ac.jp (M. Yoshimi), Kenshi.Hayakawa@kaneka.co.jp (K. Hayakawa), chikara.furusawa@riken.jp (C. Furusawa), Akihisa_Kanda@kn.kaneka.co.jp (A. Kanda), shimizu@ist.osaka-u.ac.jp (H. Shimizu).

1389-1723/$ – see front matter 
http://dx.doi.org/10.1016/j.jbiosc.2014.12.014

mitochondria (6,7). Similar results were reported in a $^{13}$C-MFA study of the CEN.PK113-7D strain cultivated in a glucose-limited chemostat culture at a dilution rate of 0.10 $h^{-1}$ (8). However, the enzyme kinetic data suggested that the PDH pathway rather than the PDC pathway should be mainly responsible for the mitochondrial acetyl-CoA supply under oxidative conditions (5–7).

In this study, to investigate the role of the PP pathway and the major route for the mitochondrial acetyl-CoA supply in the presence of a reduced Crabtree effect, $^{13}$C-MFA was performed for another experimental strain of *S. cerevisiae* S288C. The results revealed that acetyl-CoA was mainly produced via the PDH pathway in mitochondria in the presence of a reduced Crabtree effect in *S. cerevisiae* S288C. The results also showed that elevated PP pathway flux should be a common adaptation mechanism against oxidative conditions among *S. cerevisiae* strains.

## MATERIALS AND METHODS

**Strain, media, and culture conditions** *S. cerevisiae* YM1 (*MATα ura3Δ0*) was constructed from the BY4739 (*MATα leu2Δ0 lys2Δ0 ura3Δ0*) strain by restoring leucine and lysine autotrophy. The BY4739 strain was derived from S288C (9). The complete open reading frames of the *LEU2* and *LYS2* promoters together with the 335 bp and 150 bp neighboring regions were amplified using polymerase chain reaction (PCR) applied to the genomic DNA of the *S. cerevisiae* S288C strain. The PCR was performed using the following primers: for *LEU2* forward: 5′-TCATATGGATTCCTAATCCTCGAGGAGAATTTATAATATAGTCACATAACGAGAACACACAG GGGCG-3′, *LEU2* reverse: 5′-TTACCTGTATTCCTTTACATCCTCC-3′, *LYS2* forward: 5′-AGTTGCTTTCTCCTATGGGAAGAGC-3′ and *LYS2* reverse: 5′-TACAATAAACCAAGA TGAAGCTGCC-3′, respectively. PCR was performed using the Z-taq polymerase (Takara Bio Inc., Shiga, Japan). Each amplified fragment was cloned into pGEM-T easy (Promega Co., Madison, WI, U.S.A.) and was then digested by *Not*I. The fragments were transformed into the *S. cerevisiae* BY4739 strain using the lithium acetate method (10) to obtain leucine and lysine autotroph strains.

The preculture and main culture were performed in synthetic dextrose (SD) medium [5 g $L^{-1}$ glucose, 6.7 g $L^{-1}$ yeast nitrogen base without amino acids (Difco Laboratories, Detroit, MI, USA)] containing 0.076 g $L^{-1}$ uracil. Precultivation was performed at 30°C for 20 h in 5 mL of SD medium. The main culture was performed in a 1 L BNJ-P type bioreactor (ABLE, Japan) jar fermenter with a working volume of 500 mL at 30°C. The pH was maintained at 6.0 using 1*N* NaOH. The aeration rate and the agitation speed were set to 1.0 L $min^{-1}$ and 350 rpm, respectively. For the continuous culture, the dilution rate was set to 0.1 $h^{-1}$. After the continuous culture reached a steady state, the feeding medium that contained the natural glucose, was replaced with 4.93 g $L^{-1}$ glucose that contained labeled glucose composed of 41.0% [U–$^{13}$C] glucose, 30.7% [1–$^{13}$C] glucose and 28.3% natural glucose.

The cell growth and the glucose concentration were monitored using a spectrophotometer ($OD_{660}$, UVmini-1240; Shimadzu Corp., Kyoto, Japan) and a glucose sensor (BF-5; Oji Scientific Instruments, Japan), respectively. The cell dry mass was determined after centrifugation and drying at 60°C until a constant weight was achieved. The ethanol concentration was determined using a 7890A gas chromatography system (Agilent Technologies, Palo Alto, CA, USA) equipped with a capillary column (Restek 10,657 Stabilwax; 60 m × 0.32 mm ID × 1 μm; Shimadzu GLC, Japan) as previously described (11). The concentrations of glycerol, succinate, and acetate were determined using an HPLC system (HPLC Prominence, Shimadzu, Japan) equipped with an Aminex HPX-87H column (Bio-Rad, Hercules, CA, USA), a UV/VIS detector (SPD-20A), and a refractive index detector (RID-10A). The column was operated at 65°C using 1.5 mM $H_2SO_4$ as the mobile phase and with a flow rate set to 0.5 mL $min^{-1}$. The flow cell temperature of the refractive index detector was set to 35°C.

**$^{13}$C-based metabolic flux analysis** After feeding with the labeled glucose, the *S. cerevisiae* cells were sampled at 199, 201, and 203 h. The culture medium (10 ml) was centrifuged for 10 min at 10,000 rpm and 4°C. After washing with a 0.9% NaCl solution, the biomass was hydrolyzed using 6 *N* HCl at 105°C for 18 h. The hydrolyzed sample was filtered to remove cell debris and 10 μL of 600 μM cycloleucine was added as an internal standard. The sample was then dried under vacuum using an evaporator (Integrated Speedvac; Thermo Fisher scientific).The dried pellet was derivatized by adding 50 μL of acetonitrile and 50 μL of *N*-*tert*-butyldimethylsilyl-*N*-methyltrifluoroacetamide (MTBSTFA) followed by heating at 105°C for 1 h. The sample (1 μL) was analyzed by GC–MS (7890A GC and 5975C GC/MSD, Agilent Technologies) following a previously described method (12).

The metabolic network of *S. cerevisiae* was constructed using slight modifications of previously published models (2). The metabolic model comprises the major pathways of central carbon metabolism (glycolysis, PP pathway, anaplerosis, and tricarboxylic acid cycle) and the transport reaction between cytosol and mitochondria. Pyruvate, oxaloacetate, and acetyl-CoA (AcCOA) in the cytosol and mitochondria are considered to be separate metabolite pools. Alanine is synthesized from both cytosolic and mitochondrial pathways by alanine amino transferase (13). For glycine synthesis, threonine aldolase (14) accounted for by synthesis from serine. The rates of biomass synthesis were calculated from published data (15).

The computational procedure was performed by OpenMebius (16) using MATLAB (MathWorks, Natick, MA, USA). A metabolic flux distribution was estimated by a nonlinear fitting of the metabolic model using the isotopic labeling patterns of proteinogenic amino acids determined by GC–MS. The nonlinear optimization was performed by using "fmincon" function in MATLAB optimization toolbox (MathWorks, Natick, MA, USA).

The 90% confidence intervals were determined using the grid search method at the range of fixed metabolic flux whose sum of squared residuals was less than the threshold level (17). The threshold level was determined by

$$\Phi_{res,sr} \leq \Phi_{res} + \frac{\Phi_{res}}{n-p} F_{\alpha}(1, n-p) \quad (1)$$

where $\Phi_{res,\,sr}$ is the minimized squared sum of residuals with one fixed flux, $\Phi_{res}$ is the original minimized squared sum of residuals, $n$ is the number of independent data points used in the fitting, $p$ is the degrees of freedom in the original flux fit, $F$ is the $F$-distribution, and $\alpha$ is the confidence level (18).

**Mass balance analysis** ATP production through the EMP pathway and TCA cycle, together with ATP consumption by glucose uptake and phosphofructokinase, was calculated using the estimated metabolic flux distribution. The excess NADH and NADPH were assumed to be converted to ATP via oxidative phosphorylation with a P/O ratio of 1.0 as previously described (19). Several ATP consumption rates (per gram of dry cell weight, $gDCW^{-1}$) were calculated using the genome-scale model iFF708 considering growth-associated ATP maintenance, synthesis of biomass building blocks, polymerization cost, and nongrowth-associated ATP requirements (15). The amount of NADPH required for biomass formation has been estimated to be 9.31 mmol $gDCW^{-1}$ (20).

## RESULTS

**$^{13}$C-based metabolic flux analysis** In this study, $^{13}$C-MFA was performed using the YM1 strain (*MATα ura3Δ0*) constructed from the BY4739 strain that is congenic to S288C. Although the S288C strain shows slightly different metabolic phenotypes from other commonly used strains such as CEN.PK (21), the strain was employed in this study for comparison to the ATCC 32167 strain (2). The main reason for this comparison is that this is the most characterized *S. cerevisiae* strain.

A glucose-limited chemostat culture was conducted at dilution rate 0.1 $h^{-1}$ to repress the Crabtree effect. The cultivation profile (Fig. 1) showed that the culture reached a metabolic steady state at 50 h after the initiation of cultivation. The Crabtree effect was successfully suppressed because *S. cerevisiae* cells only produced a small amount of acetate (0.023 mmol $gDCW^{-1}$ $h^{-1}$) rather than ethanol and glycerol. Based on the optical density ($OD_{660}$ = 11.0) and the cell dry mass (0.21 gDCW $OD_{660}^{-1}$ $h^{-1}$), the mean glucose

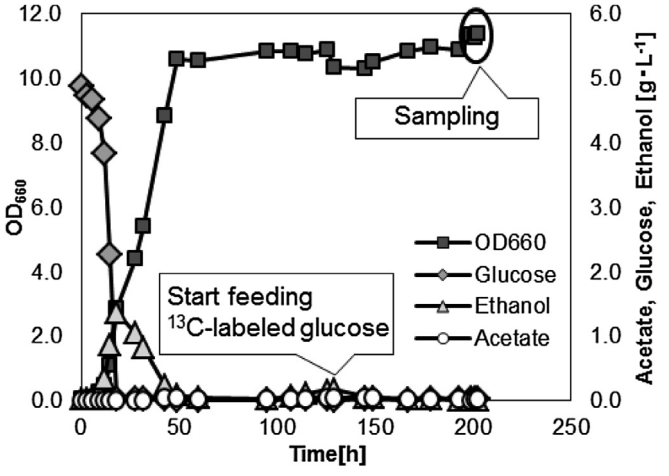


FIG. 1. Cultivation profiles. A glucose-limited chemostat culture was conducted at a dilution rate of 0.1 $h^{-1}$. The glucose-limited chemostat was performed 18 h after the culture was started. The feeding medium that contained natural glucose was replaced with labeled glucose at 129 h.

Please cite this article in press as: Kajihata, S., et al., $^{13}$C-based metabolic flux analysis of *Saccharomyces cerevisiae* with a reduced Crabtree effect, J. Biosci. Bioeng., (2014), http://dx.doi.org/10.1016/j.jbiosc.2014.12.014

uptake rate at metabolic steady state and biomass yield were determined to be 1.18 mmol gDCW$^{-1}$ h$^{-1}$ and 0.48 C-mol C-mol-glucose$^{-1}$, respectively.

At 129 h after the initiation of cultivation, the natural glucose in the feeding medium was replaced with $^{13}$C-labeled glucose. The *S. cerevisiae* cells were repeatedly sampled after the seventh resident time at 199, 201, and 203 h. In this study, three samples were considered to be three experimental replicates. Total protein was extracted from the *S. cerevisiae* cells that were hydrolyzed to a mixture of proteinogenic amino acids. Following the derivatization, the isotopic labeling patterns of each amino acid were determined by GC–MS. A metabolic flux distribution was estimated by the non-linear fitting of a metabolic model to the measured isotopic labeling patterns as shown in Fig. 2A (see Materials and methods section for the detailed procedure). The theoretical isotopic labeling patterns of the best-fitted metabolic flux distribution were similar to the measured isotopic labeling patterns, indicating that a reasonable metabolic flux distribution was estimated (see Fig. S1, Table S1). Because the measured isotopic labeling pattern data included experimental error derived from the mass analysis, there was some uncertainty in the estimated metabolic flux distribution. Thus, the 90% confidence intervals of flux levels were determined by the grid search method using the standard deviations of isotopic labeling patterns among the three experimental replicates (Fig. 2B).

**Metabolic flux distribution in *S. cerevisiae* with a reduced Crabtree effect** The $^{13}$C-MFA performed under a reduced Crabtree effect showed that the metabolic flux from glucose-6-phosphate (G6P) to glyceraldehyde-3-phosphate (GAP) via the PP pathway (72.5) was larger than that obtained via the EMP pathway (12.9). The legend of Fig. 2 defines all abbreviations for metabolites. The elevated PP pathway flux was in good agreement with that of a previous study using an ATCC32167 strain under the glucose limited chemostat cultivations at dilution rates set to 0.15 h$^{-1}$ (Fig. 2). Reproducible results were also observed for alanine and glycine biosynthesis. It has been shown that alanine and glycine are synthesized via two individual routes in *S. cerevisiae* grown on glucose as a sole carbon source (14). The metabolic flux analysis of the S288C and ATCC32167 strains commonly showed that glycine was mainly synthesized from serine, and that the mitochondrial alanine biosynthesis was more active than that originating from the cytosol (13) (Fig. 2).

The net metabolic flux (the sum of all reversible reactions) determined in this study is largely similar to that of the ATCC 32167 strain (Fig. 3) (2). However, inconsistent results were observed in the reactions responsible for the two routes from cytosolic pyruvate ($PYR_{cyt}$) to mitochondrial acetyl-CoA ($AcCOA_{mit}$) via the PDH and PDC pathways (Figs. 2 and 3). As mentioned in the introduction, the

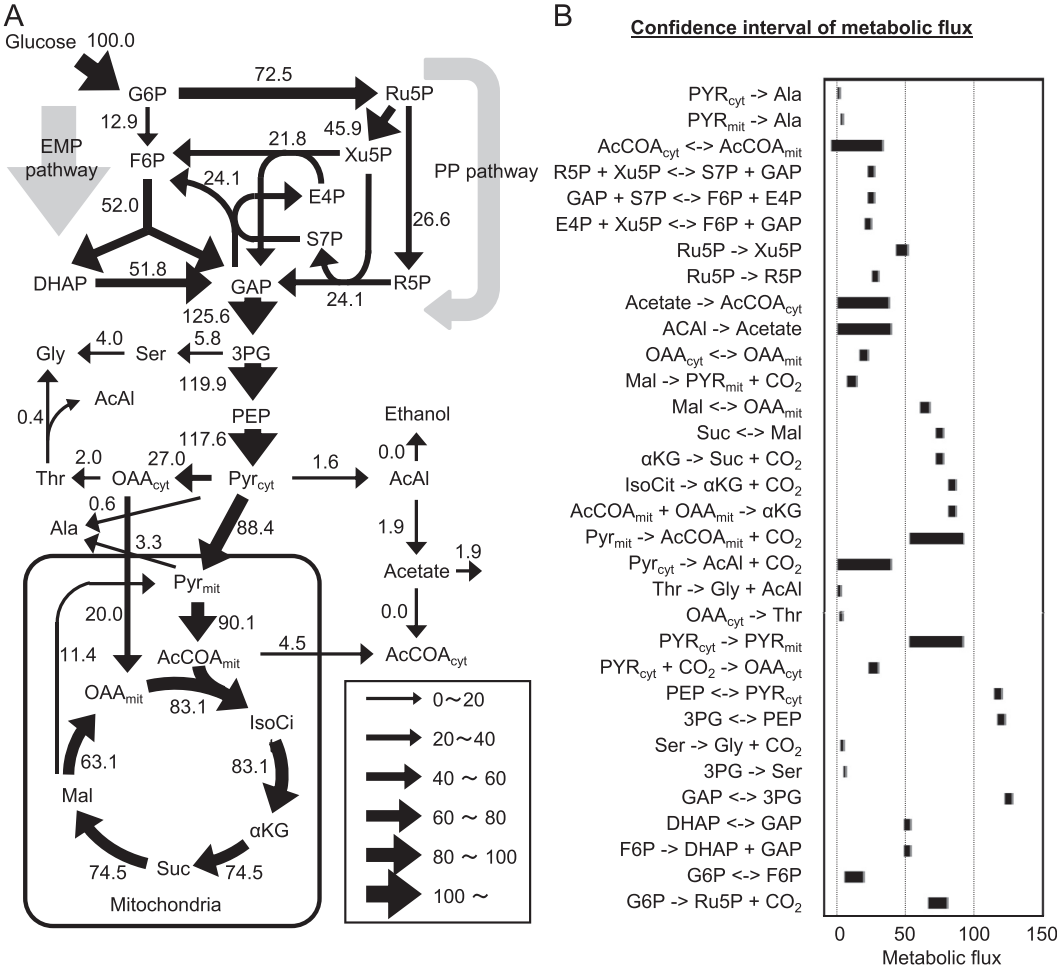


FIG. 2. Estimated metabolic flux distribution under the reduced Crabtree effect condition. (A) The normalized (relative to the specific glucose uptake rate) levels of the metabolic fluxes. (B) The 90% confidence intervals for each reaction. Suffix: cyt, localized in cytosol; mit, localized in mitochondria; metabolites: 3 PG, 3-phosphoglycerate; αKG, α-keto-glutarate; AcAl, acetaldehyde; AcCOA, acetyl-CoA; Ala, alanine; DHAP, dihydroxyacetone phosphate; E4P, erythrose-4-phosphate; F6P, fructose-6-phosphate; G6P, glucose-6-phosphate; GAP, glyceraldehyde-3-phosphate; Gly, glycine; IsoCit, isocitrate; Mal, malate; OAA, oxaloacetate; PEP, phosphoenolpyruvate; Pyr, pyruvate; R5P, ribose-5-phosphate; Ru5P, ribulose-5-phosphate; S7P, sedoheptulose-7-phosphate; Ser, serine; Suc, succinate; Thr, threonine; Xu5P, xylulose-5-phosphate.

Please cite this article in press as: Kajihata, S., et al., $^{13}$C-based metabolic flux analysis of *Saccharomyces cerevisiae* with a reduced Crabtree effect, J. Biosci. Bioeng., (2014), http://dx.doi.org/10.1016/j.jbiosc.2014.12.014

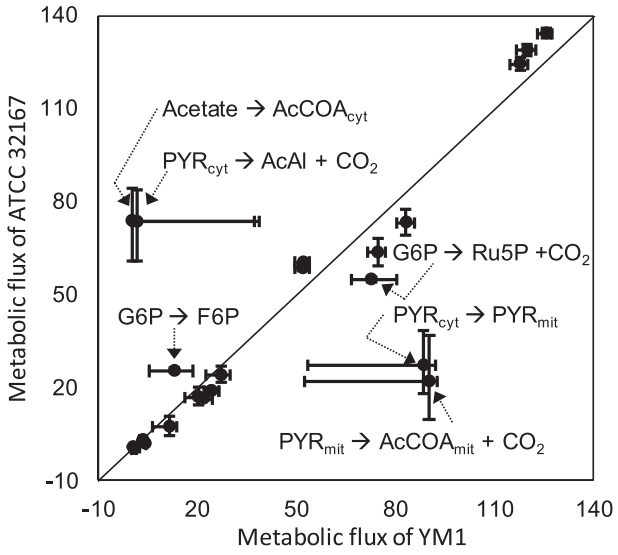


FIG. 3. Comparison of metabolic flux distribution. The X axis represents the net metabolic flux levels of the S288C derived strain estimated in this study. The Y axis indicates the metabolic flux levels of the corresponding reactions of the ATCC32167 strain obtained from the literature (2). Although the metabolic flux levels of 32 reactions were estimated in this study, 23 reactions were compared because the metabolic flux levels of 9 reactions were not estimated for the ATCC32167 strain. Error bars represent 90% confidence intervals.

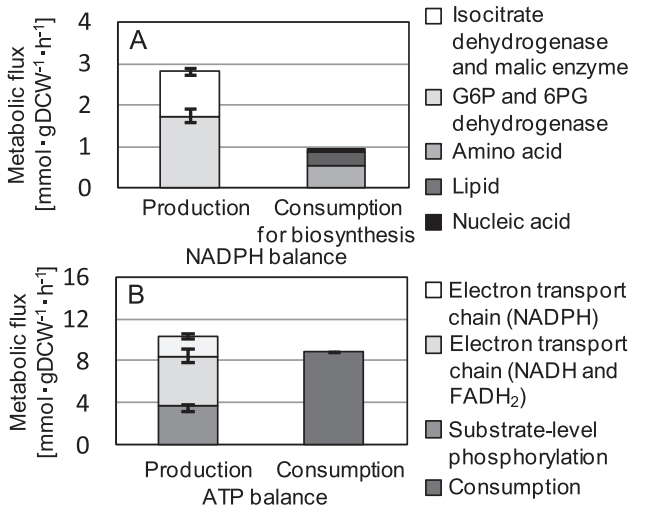


FIG. 4. Production and consumption of NADPH and ATP. The production and consumption rates (mmol gDCW$^{-1}$ h$^{-1}$) of NADPH (A) and ATP (B) were estimated using the metabolic flux distribution under the reduced Crabtree effect condition.

$^{13}$C-MFA study of the ATCC 32167 strain showed that the metabolic flux of the PDC pathway was significantly larger than that of the PDH pathway. The analysis of the S288C strain estimated the metabolic flux of the PDH pathway to be 90.1 relative to the glucose uptake rate defined at 100 (90% confidence interval: 52.1–92.5). In contrast, a rather small metabolic flux was observed for the intercompartmental AcCOA transport AcCOA cyt → AcCoA mit, The flux was estimated to be −4.5 (90% confidence interval: −4.5–32.5). Although relatively large 90% confidence intervals were estimated for these reactions, these results suggest that mitochondrial AcCOA was dominantly supplied by the PDH pathway in the S288C strain under a reduced Crabtree condition.

**Redox and ATP balance** The balance between the production and the consumption rate of NADPH and ATP were deduced from the estimated metabolic flux distribution to investigate the redox and energy states with a reduced Crabtree effect. Among the metabolic reactions potentially regenerating NADPH, the results suggested that more than 60% of the NADPH was supplied by the reactions catalyzed by G6P and 6-phosphogluconate dehydrogenase (6 PG) in the PP pathway (Fig. 4A). In contrast, the estimated NADPH consumption required for biosynthesis of nucleic acids, amino acids, and lipids (0.931 mmol gDCW$^{-1}$ h$^{-1}$) was significantly lower than the NADPH production rate (2.83 mmol gDCW$^{-1}$ h$^{-1}$), indicating that excess NADPH should be consumed by other metabolic reactions such as the respiratory chain for oxidative phosphorylation (22). ATP production was determined using the substrate level phosphorylation and the respiratory chain based on a P/O ratio of 1.0 (19). These results indicated that 64% of the ATP was supplied by the respiratory chain. In addition, the ATP balance was not closed because the estimated sum of ATP consumption (8.81 mmol gDCW$^{-1}$ h$^{-1}$) was slightly smaller than that of ATP production (10.4 mmol gDCW$^{-1}$ h$^{-1}$) (Fig. 4B).

## DISCUSSION

$^{13}$C-MFA is a useful tool to investigate mass and redox balances in microbial metabolism. Previous studies showed that the flux levels of the EMP pathway were larger than that of the PP pathway in *S. cerevisiae* ATCC 32167 and CEN.PK113-7D under the Crabtree effect (2,8). In the present study, $^{13}$C-MFA showed that mitochondrial AcCOA was dominantly supplied by the PDH pathway in the S288C strain under a reduced Crabtree condition (Fig. 2). This result was inconsistent with previous studies in which a significant role of the PDC pathway was demonstrated (Fig. 3). This discrepancy was, in part, derived from the differences in strains and experimental condition employed. Whereas the metabolic flux distribution was determined for the S288C-derived strain at dilution rate of 0.1 h$^{-1}$, $^{13}$C-MFA was conducted for the diploid strain (ATCC 32167) and a distinct experimental haploid strain (CEN.PK113-7D) at dilution rates of 0.15 h$^{-1}$ and 0.10 h$^{-1}$, respectively.

Furthermore, the large 90% confidence intervals of these reactions imply that metabolic flux analysis is inherently difficult for the PDH and PDC pathways (Fig. 2B), mainly because there is little difference in the isotopic labeling patterns of mitochondrial AcCOA (AcCOA$_{mit}$) originating from these two routes. The structure of the metabolic network indicated that relatively large flux of the malic enzyme reaction (Mal$_{mit}$ → Pyr$_{mit}$) and application of [U–$^{13}$C] glucose as the carbon source will facilitate the exact determination of these flux levels (23). Whereas the previous studies performed $^{13}$C-MFA using [1–$^{13}$C] glucose, the present study employed a mixture of natural, [1–$^{13}$C], and [U–$^{13}$C] glucose as a carbon source and a modern method to estimate confidence intervals. Although further analysis is required, the results of this study revealed that the PDH pathway could be a major route to supply mitochondrial AcCOA in *S. cerevisiae* S288C under oxidative conditions.

In *S. cerevisiae* exhibiting a Crabtree effect, a large part of the NADH that was regenerated in the EMP pathway was consumed for the biosynthesis of ethanol to maintain the NADH/NAD ratio in the cytosol, probably because the activity of NADH dehydrogenase located at the mitochondrial external membrane was insufficient for the oxidation of NADH produced at a high glucose consumption state (24,25). Substrate-level phosphorylation is inefficient in terms of the biomass yield using glucose because most of the incorporated carbon was consumed for the by-production of ethanol.

In contrast, the $^{13}$C-MFA study of the ATCC 32167 strain in the limited glucose chemostat culture demonstrated that the metabolic flux through the PP pathway was increased in the presence of a reduced Crabtree effect (2). Activation of the PP pathway was also observed in the S288C-derived strain (Fig. 2), suggesting that the

Please cite this article in press as: Kajihata, S., et al., $^{13}$C-based metabolic flux analysis of *Saccharomyces cerevisiae* with a reduced Crabtree effect, J. Biosci. Bioeng., (2014), http://dx.doi.org/10.1016/j.jbiosc.2014.12.014

elevation of PP pathway flux should be a common adaptation mechanism against oxidative conditions. Because the high biomass yield from glucose was observed in these conditions (2), the elevated PP pathway flux contributed to cell growth by supplying the required amount of NADPH.

However, the balance of the NADPH production and consumption rates, estimated from the metabolic flux distribution, was not closed (Fig. 4A). The excess NADPH is likely to be consumed by the electron transport chain because NADPH-dependent reduction of cytochrome *c* by mitochondrial extracts has been reported (22). Furthermore, the ATP balance was not closed in a strict sense when the NADPH oxidation was taken into consideration (Fig. 4B), probably because the P/O ratio may be lower than 1.0 under the reduced Crabtree effect. A decrease in the P/O ratio has been observed based on increased respiratory rate in isolated mitochondria (19), and an unknown non-growth-associated ATP requirement has also been suggested. The non-growth-associated ATP cost of the protein turnover may be larger than this estimation because the value depends on the strain and the cultivation conditions (26,27). These results suggest that an unknown mechanism for re-oxidation of cytosolic NADPH should function under oxidative conditions, and also demonstrate that the flux of the PP and EMP pathways should control the cellular metabolic state of *S. cerevisiae* via the supply of cytosolic NADH and NADPH.

Supplementary data to this article can be found online at http://dx.doi.org/10.1016/j.jbiosc.2014.12.014.

## ACKNOWLEDGMENTS

We thank Dr. Takashi Hirasawa, Dr. Katsunori Yoshikawa and Dr. Yoshihiro Toya for their helpful comments on this manuscript.

## References

1. **De Deken, R. H.:** The Crabtree effect: a regulatory system in yeast, J. Gen. Microbiol., **44**, 149–156 (1966).
2. **Frick, O. and Wittmann, C.:** Characterization of the metabolic shift between oxidative and fermentative growth in *Saccharomyces cerevisiae* by comparative $^{13}$C flux analysis, Microb. Cell. Fact., **4**, 30 (2005).
3. **Vemuri, G. N., Eiteman, M. A., McEwen, J. E., Olsson, L., and Nielsen, J.:** Increasing NADH oxidation reduces overflow metabolism in *Saccharomyces cerevisiae*, Proc. Natl. Acad. Sci. USA, **104**, 2402–2407 (2007).
4. **Diaz-Ruiz, R., Averet, N., Araiza, D., Pinson, B., Uribe-Carvajal, S., Devin, A., and Rigoulet, M.:** Mitochondrial oxidative phosphorylation is regulated by fructose 1,6-bisphosphate. A possible role in Crabtree effect induction? J. Biol. Chem., **283**, 26948–26955 (2008).
5. **Kresze, G. B. and Ronft, H.:** Pyruvate dehydrogenase complex from baker's yeast. 1. Purification and some kinetic and regulatory properties, Eur. J. Biochem., **119**, 573–579 (1981).
6. **Pronk, J. T., Yde Steensma, H., and Van Dijken, J. P.:** Pyruvate metabolism in *Saccharomyces cerevisiae*, Yeast, **12**, 1607–1633 (1996).
7. **Boiteux, A. and Hess, B.:** Allosteric properties of yeast pyruvate decarboxylase, FEBS Lett., **9**, 293–296 (1970).
8. **Gombert, A. K., Moreira dos Santos, M., Christensen, B., and Nielsen, J.:** Network identification and flux quantification in the central metabolism of *Saccharomyces cerevisiae* under different conditions of glucose repression, J. Bacteriol., **183**, 1441–1451 (2001).
9. **Brachmann, C. B., Davies, A., Cost, G. J., Caputo, E., Li, J., Hieter, P., and Boeke, J. D.:** Designer deletion strains derived from *Saccharomyces cerevisiae* S288C: a useful set of strains and plasmids for PCR-mediated gene disruption and other applications, Yeast, **14**, 115–132 (1998).
10. **Ito, H., Fukuda, Y., Murata, K., and Kimura, A.:** Transformation of intact yeast cells treated with alkali cations, J. Bacteriol., **153**, 163–168 (1983).
11. **Okahashi, N., Kajihata, S., Furusawa, C., and Shimizu, H.:** Reliable metabolic flux estimation in *Escherichia coli* central carbon metabolism using intracellular free amino acids, Metabolites, **4**, 408–420 (2014).
12. **Mori, E., Furusawa, C., Kajihata, S., Shirai, T., and Shimizu, H.:** Evaluating $^{13}$C enrichment data of free amino acids for precise metabolic flux analysis, Biotechnol. J., **6**, 1377–1387 (2011).
13. **dos Santos, M. M., Gombert, A. K., Christensen, B., Olsson, L., and Nielsen, J.:** Identification of in vivo enzyme activities in the cometabolism of glucose and acetate by *Saccharomyces cerevisiae* by using $^{13}$C-labeled substrates, Eukaryot. Cell, **2**, 599–608 (2003).
14. **Monschau, N., Stahmann, K. P., Sahm, H., McNeil, J. B., and Bognar, A. L.:** Identification of *Saccharomyces cerevisiae* GLY1 as a threonine aldolase: a key enzyme in glycine biosynthesis, FEMS Microbiol. Lett., **150**, 55–60 (1997).
15. **Forster, J., Famili, I., Fu, P., Palsson, B. O., and Nielsen, J.:** Genome-scale reconstruction of the *Saccharomyces cerevisiae* metabolic network, Genome Res., **13**, 244–253 (2003).
16. **Kajihata, S., Furusawa, C., Matsuda, F., and Shimizu, H.:** OpenMebius: an open source software for isotopically nonstationary $^{13}$C-based metabolic flux analysis, BioMed Res. Int., **2014**, 627014 (2014).
17. **Costenoble, R., Muller, D., Barl, T., van Gulik, W. M., van Winden, W. A., Reuss, M., and Heijnen, J. J.:** $^{13}$C-labeled metabolic flux analysis of a fed-batch culture of elutriated *Saccharomyces cerevisiae*, FEMS Yeast Res., **7**, 511–526 (2007).
18. **Antoniewicz, M. R., Kelleher, J. K., and Stephanopoulos, G.:** Determination of confidence intervals of metabolic fluxes estimated from stable isotope measurements, Metab. Eng., **8**, 324–337 (2006).
19. **Ouhabi, R., Rigoulet, M., and Guerin, B.:** Flux-yield dependence of oxidative phosphorylation at constant $\Delta\mu H^+$, FEBS Lett., **254**, 199–202 (1989).
20. **Bruinenberg, P. M., Waslander, G. W., van Dijken, J. P., and Scheffers, W. A.:** A comparative radiorespirometric study of glucose metabolism in yeasts, Yeast, **2**, 117–121 (1986).
21. **Kummel, A., Ewald, J. C., Fendt, S. M., Jol, S. J., Picotti, P., Aebersold, R., Sauer, U., Zamboni, N., and Heinemann, M.:** Differential glucose repression in common yeast strains in response to HXK2 deletion, FEMS Yeast Res., **10**, 322–332 (2010).
22. **Sollner, S., Deller, S., Macheroux, P., and Palfey, B. A.:** Mechanism of flavin reduction and oxidation in the redox-sensing quinone reductase Lot6p from *Saccharomyces cerevisiae*, Biochemistry, **48**, 8636–8643 (2009).
23. **Christen, S. and Sauer, U.:** Intracellular characterization of aerobic glucose metabolism in seven yeast species by $^{13}$C flux analysis and metabolomics, FEMS Yeast Res., **11**, 263–272 (2011).
24. **Larsson, C., Pahlman, I. L., Ansell, R., Rigoulet, M., Adler, L., and Gustafsson, L.:** The importance of the glycerol 3-phosphate shuttle during aerobic growth of *Saccharomyces cerevisiae*, Yeast, **14**, 347–357 (1998).
25. **Rigoulet, M., Aguilaniu, H., Averet, N., Bunoust, O., Camougrand, N., Grandier-Vazeille, X., Larsson, C., Pahlman, I. L., Manon, S., and Gustafsson, L.:** Organization and regulation of the cytosolic NADH metabolism in the yeast *Saccharomyces cerevisiae*, Mol. Cell Biochem., **256–257**, 73–81 (2004).
26. **Hong, K. K., Hou, J., Shoaie, S., Nielsen, J., and Bordel, S.:** Dynamic $^{13}$C-labeling experiments prove important differences in protein turnover rate between two *Saccharomyces cerevisiae* strains, FEMS Yeast Res., **12**, 741–747 (2012).
27. **Lahtvee, P. J., Seiman, A., Arike, L., Adamberg, K., and Vilu, R.:** Protein turnover forms one of the highest maintenance costs in *Lactococcus lactis*, Microbiology, **160**, 1501–1512 (2014).

Please cite this article in press as: Kajihata, S., et al., $^{13}$C-based metabolic flux analysis of *Saccharomyces cerevisiae* with a reduced Crabtree effect, J. Biosci. Bioeng., (2014), http://dx.doi.org/10.1016/j.jbiosc.2014.12.014